Langmuir

Article

pubs.acs.org/Langmuir

Thermodynamically Stable Dispersions of Quantum Dots in a Nematic Liquid Crystal

Maksym F. Prodanov,[†] Nataliya V. Pogorelova,[†] Alexander P. Kryshtal,[†] Andrey S. Klymchenko,[‡] Yves Mely,[‡] Vladimir P. Semynozhenko,[†] Alexander I. Krivoshey,[†] Yurii A. Reznikov,[§] Sergey N. Yarmolenko,[∥] John W. Goodby,[⊥] and Valerii V. Vashchenko*[,†]

[†]State Scientific Institution "Institute for Single Crystals", NAS of Ukraine, 60, Lenin Ave., Kharkov, 61001, Ukraine

[‡]Faculty of Pharmacy, UMR CNRS 7213, University of Strasbourg, Strasbourg, France

[§]Institute of Physics, NAS of Ukraine, 46, Nauki Ave., Kiev, 03039, Ukraine

[∥]North Carolina A&T State University, Greensboro, North Carolina 27411, United States

[⊥]Department of Chemistry, University of York, York YO10 5DD, United Kingdom

Supporting Information

ABSTRACT: Using transmittance electron microscopy, fluorescence and polarizing optical microscopy, optical spectroscopy, and fluorescent correlation spectroscopy, it was shown that CdSe/ZnS quantum dots coated with a specifically designed surfactant were readily dispersed in nematic liquid crystal (LC) to form stable colloids. The mixture of an alkyl phosphonate and a dendritic surfactant, where the constituent molecules contain promesogenic units, enabled the formation of thermodynamically stable colloids that were stable for at least 1 year. Stable colloids are formed due to minimization of the distortion of the LC ordering around the quantum dots.

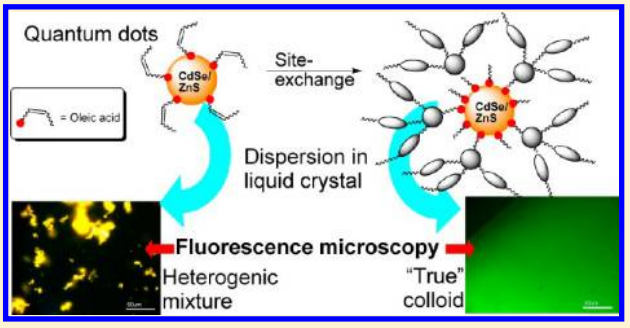

INTRODUCTION

The prospect of combining the unique properties offered by various inorganic nanoparticles (NPs) with the remarkable responsive properties of liquid crystals (LCs) is of intense interest.[1−5] For example, doping LCs with magnetic NPs is a promising route toward enhancing the sensitivity of LCs in response to external fields,[6−12] and dispersions of ferroelectric NPs are characterized by an increase in the dielectric anisotropy and birefringence of the LC host system.[9,13−15] Other types of NPs such as those based on noble metals[16−22] and semiconductors, quantum dots (QD) or rods,[3−5,23−40] dispersed in liquid crystal hosts also affect mesogenic ordering, optical, dielectric, and electro-optic properties of the resulting colloidal materials. Of particular interest are dispersions of QDs in LCs as the polarization[24] and intensity[25,27,29] of their luminescence, and other optical properties can be manipulated via the application of external electric fields.[3,23,24,31−35,37−40]

Despite the great interest in colloidal dispersions of NPs in liquid crystal host systems, fundamental research and the development of applications that utilize this new class of materials is often hampered by the strong tendency of nanoparticles to aggregate in the liquid crystal host, an effect which typically much more pronounced than in the corresponding isotropic liquid of the host employed.

Indeed, the stability of dispersions formed by NPs in LC hosts is typically poor and is almost irrespective of the types of NPs employed.[3−8,11,15−17,22,26,30−32,37−43] Moreover, the aggregates formation often occurs even in colloids with low-content of NPs (see, e.g., ref 4 and references cited therein). The origin of this instability depends on the size of the particles. For rather large particles, $d_{part} \geq 100$ nm, distortions of the director of the LC around the particles are necessitated. These distortions give rise to attractive orientational elastic forces between the particles, which encourage aggregation. Small nanoparticles, with size $d_{part} \ll 100$ nm, do not disturb the director of a LC because it requires too much energy, and therefore orientational elastic forces do not notably contribute to the aggregation process. In this case, interactions due the change of the order parameter near the particles come to play an important role. To compensate for distortions of the order parameter around the particles, the NPs approach each other as long as particles are at a distance of tens nanometers from each other.[44] This general effect encourages aggregation of any kind of nanoparticles in a LC phase, and makes the problem of aggregation more severe than in isotropic solvents.

In order to decrease aggregation, surfactants are used to coat the surface of the nanoparticles. It is traditionally thought that the role of surfactant is to increase the excluded volume (in other words, to increase the steric repulsion radius) of the NPs. Another role of surfactants is to "smooth out" the disturbance

Received: April 18, 2013
Revised: June 21, 2013
Published: June 28, 2013

   dx.doi.org/10.1021/la401475b | Langmuir 2013, 29, 9301−9309

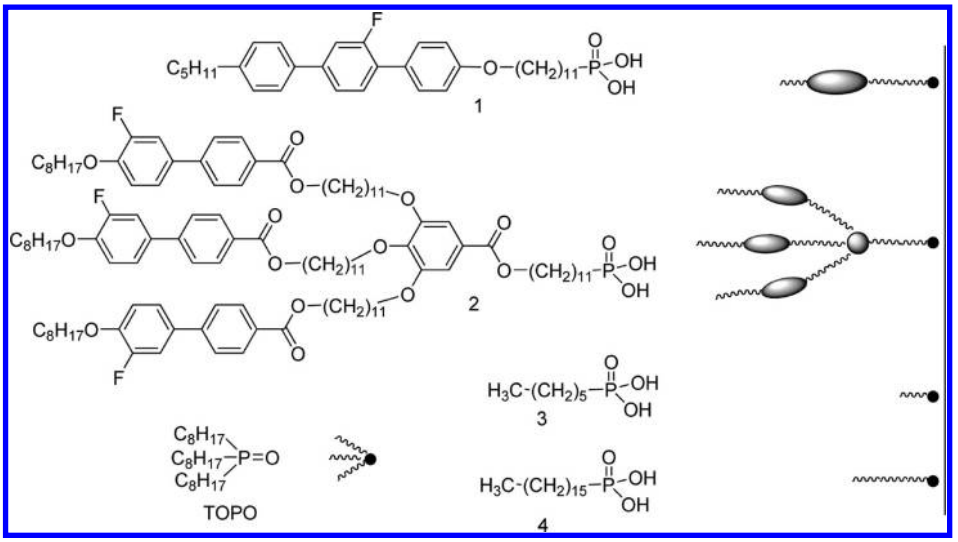

Figure 1. Structures of the surfactants **1**−**4** and their relative dimensions.

of the local director of the LC caused by the particles. Therefore, it is not a coincidence that most stable colloidal liquid crystals are achieved using either surfactants composed of molecules with promesogenic structures or a combination of promesogenic surfactants and aliphatic ligands.[16,19−22,40,43] However, the influence of surfactant structure on the stability of the colloids in mesophases has not been studied extensively to date. Furthermore, the lack of reliable methods to study the aggregation of NPs in LC hosts additionally complicates these studies.

Herein we demonstrate that it is critical to optimize the interactions between the molecules of the LC matrix and the surface coatings of the nanoparticles in order to avoid aggregation of the NPs, thereby producing truly stable colloidal systems. We achieved such colloidal systems using specially coated quantum dots of CdSe/ZnS dispersed in the nematic host, 4-pentyl-4′-cyanobiphenyl (5CB). The luminescent nature of QDs provides an opportunity to visualize the degree to which aggregation of NPs occurs in the LC host via the use of fluorescence detection techniques, such as fluorescence microscopy (FM, similar to refs 3, 17, 32, 33, and 38) and fluorescence correlation spectroscopy (FCS). As the FCS signal is acquired from luminescent objects only, this methodology has an advantage over the more general technique of dynamic light scattering (DLS), where strong fluctuation of the director complicate data interpretation. Both FCS and DLS methods are widely applied to study different kinds of NPs dispersions in isotropic media. In the case of LC colloids, however, there are only few examples of the application of DLS[31] and, to the best of our knowledge, there are no studies that describe the use of FCS.

EXPERIMENTAL SECTION

In order to stabilize the formation of colloids composed of quantum dots in nematic liquid crystals, it is necessary to design and prepare organic ligands (surfactants) with specific structures, topologies, and properties. The synthesis of the materials is described fully in the Supporting Information; here we discuss the molecular design of the materials to be investigated.

The choice of QDs was dictated by the use of fluorescence microscopy and fluorescence correlation spectroscopy in our studies. Specifically, the excitation range of the QDs should be sufficiently shifted from the excitation of the luminescence of the host nematic material, 5CB.

Two types of CdSe/ZnS QDs were synthesized:[45] green-emitting quantum dots **QD1** (maximum of the photoluminescence at λ_{em} = 530 nm, quantum yield, $\eta_{em} \approx 30\%$) and yellow-emitting quantum dots **QD2** (λ_{em} = 573 nm, η_{em} = 17%). The photoluminescence of both types of QDs can be excited by irradiation in the range of 400−480 nm, and their mean diameter was 3.5 nm. The synthesized QDs were coated with a hydrophobic shell; according to literature data, it consists of mixture of aliphatic-based compounds (so-called "native" surfactants), which were oleic acid and trioctylphosphine oxide (TOPO), presumably with small amounts of octylphosphonic acid.[46]

After the fabrication of the QDs, their "native" surfactant covering was replaced with the two types of new surfactants (Figure 1): (i) a linear surfactant possessing a terphenyl promesogenic moiety (a "single core" surfactant, **1**)[47] which has been recently applied in the stabilization of Fe_3O_4 dispersions in smectic LCs[43] and (ii) a dendritic surfactant, **2**, with three promesogenic biphenyl units.

Furthermore, two types of alkylphosphonic surfactants, 1-hexylphosphonic acid (**3**) and 1-hexadecylphosphonic acid (**4**), were used to vary the density of the surfactants **1** and **2** on the surface of the NPs. We therefore targeted the incorporation of one to two molecules of the cosurfactant (**3** or **4**) between molecules of the main surfactants **1** or **2** on the surface of each QD. Mixtures with a 2:1 ratio of the surfactants **3** and **1** and a 4:1 ratio of the surfactants **3** and **2** were used. This ratio was selected by taking into account the larger diameters of the molecules of the surfactant **2** relative to those of the surfactant **1**, and the corresponding differences in their footprint areas on the surfaces of the QDs.

The surfactants **1**−**4** were linked to the QDs surfaces through phosphonic acid groups. These groups have a strong affinity for the CdSe/ZnS surface and, contrary to traditional terminal thiol functions,[48,49] do not decrease the quantum yields of photoluminescence significantly.[49−51] The affinity of phosphonic acids groups to QD surfaces also exceeds that of other popular terminal groups such as carboxylic acids or phosphine oxides.[46,48,49]

The site-exchange was achieved via prolonged heating of the NPs in toluene under an argon atmosphere with an excess of the appropriate surfactant(s). The quantum yields of resurfaced QDs were reduced by no more than half that is within the general tendency for site-exchange procedures.[52] Qualitatively the progress of the site-exchange was monitored by FT-IR spectroscopy and energy dispersive X-ray spectroscopy (EDX-spectroscopy). The FT-IR spectral evolutions upon grafting of the QDs and accompanied changes in elemental contents are given in the Supporting Information.

Here after, the fabricated NPs are referred as **QD1-1**, **QD1-2**, **QD1-1-3**, **QD1-2-3**, **QD1-2-4**, and **QD2-2-3** (see Figure 2), where the first

dx.doi.org/10.1021/la401475b | Langmuir 2013, 29, 9301−9309

number in the abbreviation, denotes the type of QD used, and the second and third numbers indicate the type of ligands employed (see Figure 2).

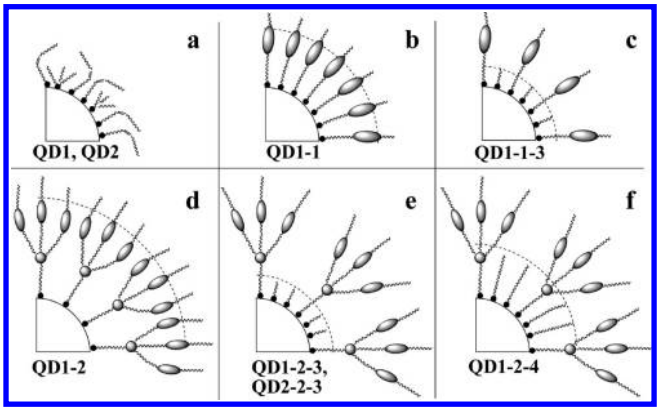

Figure 2. Schematic representation of the QDs grafted with the surfactants (to scale): (a) the native surfactant and (b–f) the new surfactants. The dotted lines illustrate a possible depth of penetration of 5CB molecules into the QDs shell.

In order to prepare dispersions of the QDs in a LC, a dispersion of QDs in toluene was added to a 5CB (clearing temperature $T_c \approx 34.5$ °C) and the toluene was removed using stream of argon at an elevated temperature, drying in vacuo and sonication where necessary. The feed concentration of QDs in 5CB was approximately 0.25 wt %. The textures of the dispersions observed by polarizing optical microscopy (POM) are similar to those observed for pure 5CB between untreated glass substrates regardless whether the QDs were aggregated in the dispersion or not. However, the available glass substrates and coverslips provide homeotropic alignment of LC for all the samples including pure 5CB. Therefore, in this case, it is difficult to judge if the vertical alignment is induced by NPs similarly as it was observed recently.[43]

All of the samples were subjected to fluorescence microscopy (FM) equipped with CCD-camera and fiber-optical spectrometer which was used to record the emission spectra. For the representative dispersions (see Table 1), the data obtained by fluorescence microscopy was in good agreement with the results obtained from two-focus fluorescence correlation spectroscopy (FCS).[53] Due to the requirements of the FCS setup, the concentration of the QDs in the sample investigated was around 0.0025%, that is, 2 orders of magnitude less than in the experiments described above.

Table 1. Results of FCS Measurements (τ_{QD}), the Estimated Diameter of QDs (d_{QDs}), and Checking for Aggregates Presence by Confocal Microscopy for the LC-QDs Colloids and the Reference Sample

	TMR	QD2	QD1-1	QD1-2	QD1-2-3	QD2-2-3
correlation time, τ_{QD}, ms[a]	0.038	721	8.7	12.9	8.6	9.9
diameter, d_{QDs}, nm	1.2	812	9.8	14.5	9.7	11.1
aggregation[b]		+++	+	++	−	−

[a]The measurements were carried out for T = 300 K. [b]"+" or "−" denotes the presence or absence of aggregates; number of "+" qualitatively characterizes the degree of aggregation.

In the FCS technique, the correlation time of fluctuations of fluorescence femtoliter excitation volume are monitored, and the resulting correlation time (τ) of the fluorescence signal is used to determine the diffusion coefficients of the fluorescent objects.

FCS measurements were carried out for the reference fluorescent species 5-carboxytetramethylrhodamine (TMR) in water (diffusion coefficient, D_{TMR} = 421 μm^2 s^{-1}; see ref 2 in the Supportring Information) and for our QDs in 5CB. The measured values of τ allowed us to estimate the hydrodynamic diameter, d_{QDs}, of the QDs from the Stokes–Einstein equation:

$$d_{QDs} = k_B T/3\pi\eta D_{QDs} = k_B T/[3\pi\eta D_{TMR}(\tau_{TMR}/\tau_{QDs})] \quad (1)$$

where k_B is the Boltzmann constant, η is the viscosity of the LC (26 mP·s),[54] and τ_{TMR} and τ_{QDs} are the correlation times of TMR and the QDs, respectively. FCS is a very sensitive technique to monitor QDs aggregation, as the correlation time is proportional to the particle size. However, we should admit that the resolution of the FCS based on the correlation time is limited, as the formation of very small aggregates, such as dimers of QDs, would not be possible to detect because of very limited change in the particle size (cube root of the particle mass).

It should be noted that eq 1 does not take into account anisotropic diffusion of the particles in the nematic host. However, since our particles do not disturb the director of the LC, their diffusion can be considered to be similar to the diffusion of molecular dopants, for which the value of the diffusion anisotropy is typically small (~30%).[55] Furthermore, in our case, unaligned LC samples were used, and the average effective diffusion coefficient $1/3D_{\parallel} + 2/3D_{\perp}$ (the indices denote the diffusion coefficients along and perpendicular to the director) was measured. Therefore, the anisotropy of the diffusion should not significantly affect our estimations of the effective size of the QDs. Our FCS analysis also does not account for blinking of QDs. According to the previous reports, the QDs blinking and other anomalous behaviors, which become important for higher excitation powers, may influence the amplitude of the autocorrelation function with only limited effect on the correlation time.[56] Therefore, the correlation time is sufficiently robust parameter to estimate the size of the dispersed QDs. A detailed description of the FCS setup[57] and the analysis used is given in Supporting Information.

The method used to prepare TEM samples was similar to the method described in ref 43, and it allowed for the direct observation of the QDs aggregates in the LC matrix. Briefly, a dispersion of the QDs in the LC was smeared on a TEM grid without any dilution with volatile solvent and used for image acquisition; see Figure 4. (See also the Supporting Information.)

RESULTS

Initially, dispersions of the NPs coated with native surfactants, **QD2**, in the 5CB were examined in order to provide baseline dispersions for comparative studies. Dispersions that contained residual toluene appeared optically homogeneous. However, after full removal of the solvent, luminescent heterogeneities, visible to the naked eye, formed quickly in the dispersion. Treating the dispersion with powerful ultrasound (22.5 kHz, ~500 W output) at an elevated temperature (~70 °C) restored it to a uniformly colored material, however, only for a period of several hours.

Under fluorescence microscopy, even freshly restored and sonicated samples of **QD2**, filled in planar glass capillaries (thickness, L = 5–10 μm), looked like a dispersion of micrometer sized, yellow emitting objects of irregular shape and sizes (see Figure 3a).

The luminescence spectrum taken from an area enriched with the objects (insert at Figure 3a) almost coincided with the spectrum of the **QD2** colloid in toluene; that is, these objects can unambiguously be assigned as aggregates of the nanoparticles. The areas between the aggregates showed almost no luminescence, thereby suggesting that these areas contain a negligibly low concentration of QDs. The FM observations were confirmed by the data obtained from FCS studies in which, despite two-order dilution of the colloid, only fluorescent objects of micrometer size were detected (see Table 1). These objects were also observed in the confocal

dx.doi.org/10.1021/la401475b | Langmuir 2013, 29, 9301–9309

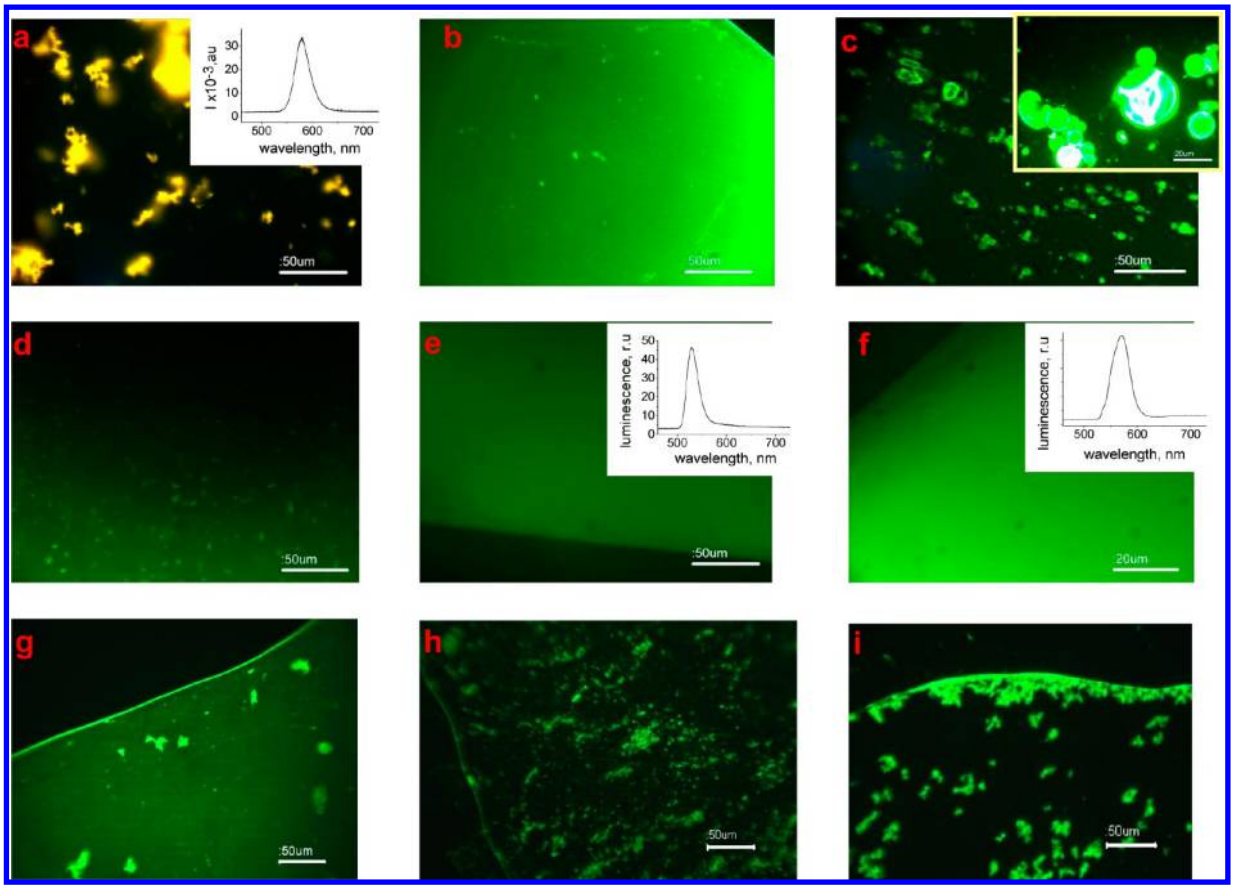

Figure 3. Fluorescence microscopy images ($\lambda_{exitation}$ 450 − 480 nm) of the 0.25 wt % dispersions in 5CB of (a) as-synthesized **QD2** (coated with "native" surfactants); (b) **QD1** grafted with surfactant **1** (sample **QD1-1**); (c) **QD1** grafted with surfactant **2** (**QD1-2**); the inset shows the same sample at higher magnification. (d−i) QDs covered with mixtures of surfactants: (d) **QD1-1-3**; (e) **QD1-2-3**; (f) **QD2-2-3**; (g) **QD1-2-3** where **2** and **3** were taken in 1:8 ratio; (h) **QD1-2-4** where **2** and **4** were taken in 1:4 ratio; and (i) **QD1-2-4** where **2** and **4** were taken in 1:8 ratio; the green color of the yellow-emitting particles (f) is an optical illusion that occurs due to a mixture of the residual pump light (blue) and fluorescence light (yellow). For confirmation, see the UV spectrum on the figure inset; insets in (a), (e) and, (f) show the emission spectra acquired from the center of the emitting area; in (e−i), sample edges (black areas) are shown in order to confirm the focus and to guide the eye.

microscope equipped with the FCS setup (see Supporting Information, Figure S7).

Thus, the QDs coated with aliphatic surfactants are only capable of forming short-lived, micrometer-sized suspensions in the LC before aggregation occurs. Since the formation of large aggregates was observed even in quite diluted colloids, the following study was focused on low-concentrated colloids so far.

Conversely, the promesogenic surfactants, both with a linear structure, **1**, and with a dendritic structure, **2**, applied individually to the QDs enhance homogeneity of the dispersions. Freshly prepared dispersions of the QDs coated with these surfactants in 5CB appeared to be optically homogeneous to the naked eye, even without sonication. The suspensions stabilized with the individual surfactants **1** and **2** maintained their homogeneity for approximately 24 h, after which time QDs aggregates became visible by eye, and ultimately precipitation occurred. However, the precipitated aggregates could be readily redispersed by heating the heterogeneous mixture to 60−70 °C with gentle agitation for approximately 1 min. This redispersion effect is naturally explained by the absence of order-induced interactions between the aggregated nanoparticles in the isotropic phase of the LC host.

Despite the apparent optical homogeneity to the naked eye, more detailed examinations revealed that dispersions of QDs coated with single promesogenic surfactants showed a certain degree of aggregation in the case of the linear surfactant **1** (sample **QD1-1**) and a greater degree of aggregation in the case of the dendritic surfactant **2** (sample **QD1-2**).

For example, upon examination of the samples by FM, **QD1-1** showed almost uniform emission with a few bright colored points (Figure 3b). Luminescence spectra taken from random areas of the sample were found to be very similar to those obtained from dispersion in isotropic solvent, thereby indicating that the LC has a negligibly small effect on the emission of the QDs.

The spatially uniform emission of our colloids implies that the characteristic scale of optical inhomogeneities within the sample is much less than the wavelength of the emission light, that is, <500 nm. In other words, the size of any aggregates within the samples well as distances between them in the uniform emission areas is much less than 500 nm. In the case of a stable, not-aggregated colloid, the mean distance between the QDs is expected to be approximately 90 nm (see the Supporting Information, chapter 5.1). We can therefore assume that a "true" colloidal dispersion is formed in the areas of the **QD1-1** sample that show uniform emission.

dx.doi.org/10.1021/la401475b | *Langmuir* 2013, 29, 9301−9309

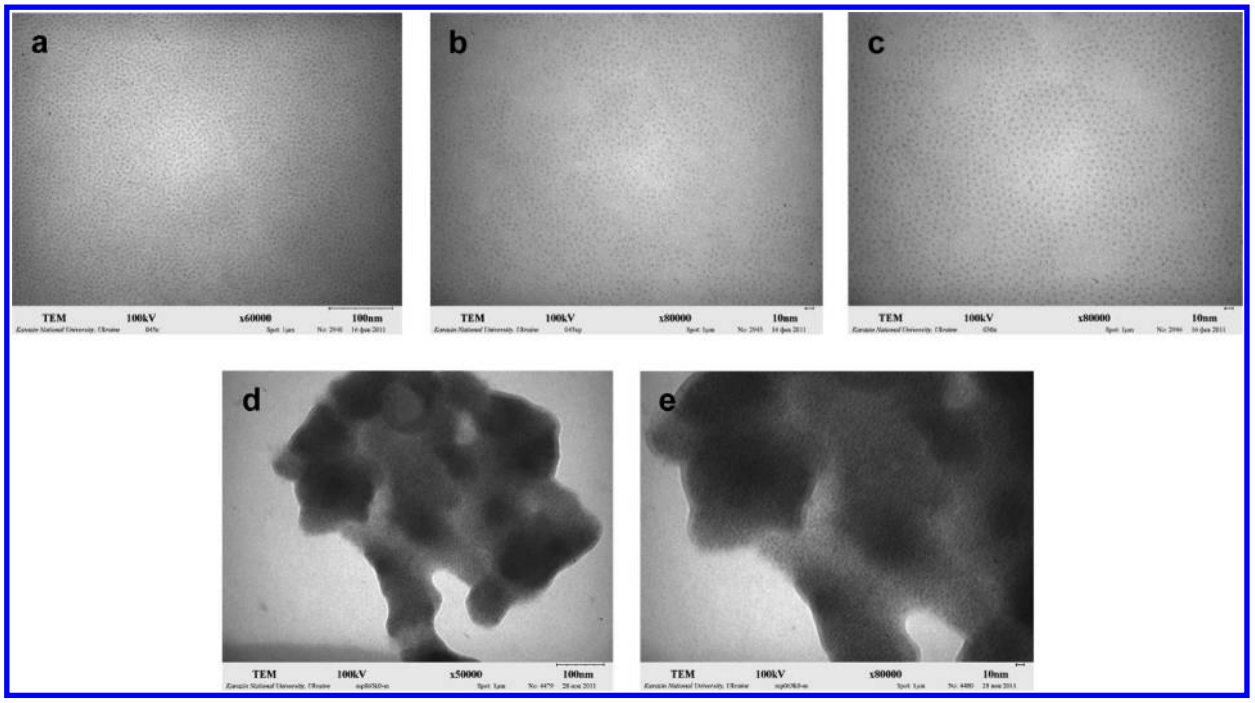

Figure 4. TEM images of the 0.25 wt % dispersions in 5CB of (a, b) **QD1-2-3**; (c) **QD2-2-3**; (d, e) **QD1**.

In the case of **QD1-2** dispersions, a number of green-emitting objects were observed by fluorescence microscopy. The areas between the aggregates were found to exhibit a luminescence intensity which was much weaker than in the case of **QD1-1**, thereby indicating that the concentration of nonaggregated QDs in these regions is lower than in the analogous regions within dispersions of **QD1-1** (Figure 3c). At higher magnifications, these objects appear as liquidlike droplets rather than solid inclusions (cf. Figure 3c with a). The presence of these liquidlike droplets might be a sign of inherent mesomorphism of **QD1-2** material, as observed for similar mesogen-coated NPs.[58,59] However, in order to confirm this suggestion, additional studies are required.

In each of the dispersions of QDs decorated with the promesogenic surfactants (**QD1-1** and **QD1-2**), the simultaneous presence of separate QDs (with a size of the order of 10 nm) and their aggregates (visible by confocal FM) was also detected by FCS studies (see Table 1 and Supporting Information, Figure S7).

Thus, both of the promesogenic surfactants, **1** and **2**, essentially decrease the tendency of the QDs to aggregate in the LC, although a small degree of aggregation still occurs. It is worth noting that linear surfactant **1** suppresses aggregation more effectively than the dendritic surfactant (**2**), although it was expected that the latter would better facilitate interactions between the outer shell of QDs and the surrounding LC matrix.

In order to enhance the interactions between the LC and the surfactant shell, and therefore obtain a stable colloidal system, we attempted to "smooth out" the disturbance of the LC order parameter around the particles by increasing the contact area between the molecules within LC phase and the molecules of the surfactant coating. We achieved this by incorporating short-length cosurfactants **3** or **4** between molecules of the main surfactants **1** or **2** (Figure 2c,f). Recently it was shown that gold NPs with a similar architecture of stabilizing shell are capable to form stabile dispersions in LC matrices (refs 18−20, ref 11 in ref 19, and ref 60).

The colloid of **QD1-1-3** in 5CB (Figure 3d) showed similar fluorescence microscopic patterns to the dispersion of QDs stabilized with surfactant **1** (Figure 3b and Supporting Information, Figure S7e); that is, the "thinning" of the linear promesogenic surfactant with the short-length cosurfactant does not significantly affect the extent of aggregation. In contrast, the colloidal systems of **QD1-2-3** and **QD2-2-3** appeared uniform emitting (Figure 3e and f) by FM, and we have not observed any signs of aggregation in these samples in over a year. Moreover, the fluorescence spectra, randomly acquired from different emitting areas of the microscopic pattern, did not differ from the fluorescence spectra of the NPs in an isotropic solvent (see insets in Figure 3e and f). The sizes of fluorescent species, as determined by FCS (Table 1), are also comparable with the expected size of the separate QDs particles; the diameter of the bare QDs is 3.5 nm, and the size of the surfactant coating is 4−6 nm. These data therefore strongly suggest that "true" colloidal systems have been achieved in the case of dendritic surfactant **2** coatings "thinned" with the short-length cosurfactant **3** in 1:4 ratio.

The stability of the colloid requires a delicate balance between the surface concentration and the relative lengths of the main dendritic promesogenic surfactant and aliphatic cosurfactant. A too strong dilution of the dendritic surfactant **2** with the aliphatic species **3** (1:8 ratio) results in appearance of NPs aggregates (see Figure 3g). The same effect is observed when the short-chain cosurfactant **3** is replaced by longer homologue (**4**) (cf. Figure 3e,f with h and i).

In addition to the data acquired from static FM and FCS studies, the notion that both **QD1-2-3** and **QD2-2-3** form thermodynamically stable colloidal dispersions in 5CB is also supported by TEM studies; that is, a small amount of the dispersion of the NPs in the LC was smeared directly on to a TEM grid, without any dilution with solvent, and images were taken[43] (see Figure 4).

The QDs covered with the "native" surfactant (**QD1**) are bundled into irregular shaped clumps mediated by areas that

dx.doi.org/10.1021/la401475b | *Langmuir* 2013, 29, 9301−9309

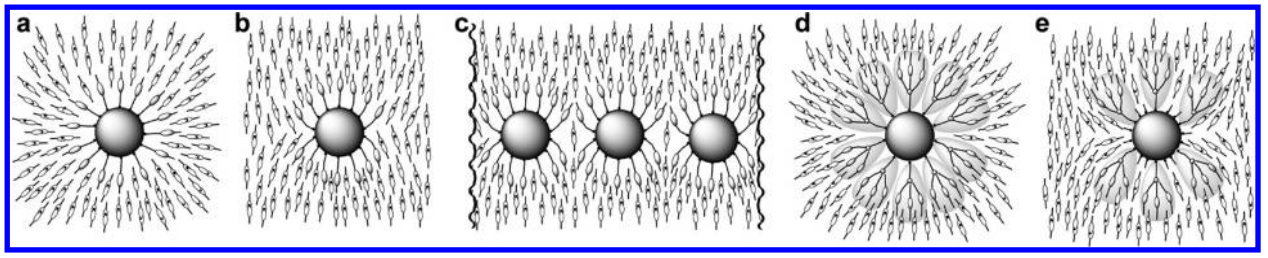

Figure 5. Schematic representation of QDs in 5CB: (a) **QD1-1** in isotropic phase; (b) **QD1-1** in nematic; (c) possible type of **QD1-1** aggregation in nematic; (d) **QD1-2** in nematic; (e) **QD1-2-3** in nematic.

are almost free of clustering (Figure 4d,e). Conversely, the quantum dots **QD1-2-3** and **QD2-2-3** coated with the mixed dendritic/aliphatic surfactants are uniformly distributed over the grid (Figure 4a–c). The differences between the two types of TEM pattern can be rationalized if we suppose that the LC matrix is evaporated in high vacuum in the TEM chamber (10^{-7} Torr), and that suspended NPs are deposited onto the copper grid. In such a way, the colloids of QDs with modified surfaces that are well dispersed in the LC matrix produced uniformly covered TEM patterns upon drying (see Figure 4a–c), whereas the crude dispersions of QDs that aggregated (as also observed by FM at Figure 3a), dried out into irregular spots on the TEM grid, without of the possibility of redispersion (see Figure 4d, e). This indicates that, in these systems, the QDs are homogeneously distributed within the LC matrix, as it was also concluded from the FM and FCS data. A detailed analysis of TEM images is given in the Supporting Information.

DISCUSSION

Thus, the experimental data allow us to conclude that the best stability of the colloids was obtained for QDs coated with the promesogenic dendritic ligand thinned with a short aliphatic surfactant. Moreover, thermodynamically stable colloids were obtained for these kinds of QD shells.

The obtained results can be explained in terms of the distortion in the local ordering of the LC host caused by the particles and their surfactant shells. As was noted in the introduction, the tendency of nanoparticles to aggregate in a LC matrix is always much stronger than in an isotropic environment. Obviously, this effect is caused by the orientational ordering of the constituent molecules within the mesophase. Since the sizes of the considered nanoparticles (≈3.5 nm) and the surfactant coatings (≈4–6 nm) are of the order of the length of 5CB (≈ 1.6 nm), a macroscopic approach and consideration of the problem in the terms of LC director are not valid. Therefore, it follows that we cannot consider directly the interaction of the particles with the LC host in terms of the anchoring of the director at the particle surface and orientational elastic forces. Instead, LC-NP interaction must be considered on a molecular level, thereby taking into account the local orientational ordering of the surfactant and LC molecules within the surfactant shell and in the vicinity of the particles.

In accordance with this approach, the nanoparticles disturb the local ordering of the LC around them and, in turn, the interactions between the LC and surfactant molecules impose a degree of orientational ordering within the surfactant shell[19] such that the ligands are oriented to be parallel to the local director field. Such alignment of cyanobiphenyl ligands was recently detected in suspensions of 4 nm Au particles in 5CB by wide-line ^{2}H NMR spectroscopy.[61] Thus, the shape of the coated nanoparticles will no longer be spherical, as it would be in the isotropic phase (Figure 5a), but will instead be tactoidal (Figure 5b). In such a way, the mutual ordering of the LC molecules and surfactant molecules minimizes the orientational energy of the system and decreases the distortion of the local director field around the NPs. This effect is more pronounced when the surfactant molecules are structurally compatible with the LC host, that is, when the ligands bear promesogenic units and when the structure of the nanoparticle shell allows the penetration of the constituent molecules of the LC between the molecules of the surfactant. Smaller distortions of the LC around the particles lowers their propensity to aggregate, thereby enhancing the stability of the colloid.

This conclusion is in agreement with our results. QDs coated with the dendritic surfactant **2** diluted with the short aliphatic surfactant **3** (**QD1-2-3** and **QD2-2-3**) forms a "true" colloid with no traces of aggregation. The structure of the shell in this case provides a large amount of space for the molecules of LC. Additionally, three promesogenic units within the structure of the main surfactant **2** guarantee effective interaction with the molecules of the nematic host (Figure 5e). With regard to the importance of the relationship between the lengths of the main dendritic surfactant **2** and cosurfactant, it is clear that the application of the short (half-length of the main surfactant spacer, see Figures 1 and 2c, e) cosurfactant **3** resulted in the formation of a "true" colloid, whereas the chains of the surfactant **4** molecules are too long (one-third longer than spacer in **2** and **3**, Figures 1 and 2f) to allow the effective penetration of the LC host molecules into the shell and therefore aggregation is observed (cf. Figure 3h and i).

Despite the similar structure of the NPs shell in the case of both **QD1-2-3** and **QD1-1-3**, the interaction of the linear surfactant **1** (one promesogenic unit per anchoring group) with the constituent molecules of the LC host is not as effective as it is in the case of the dendritic surfactant **2**, which contains three promesogenic units within the molecular architecture. Instead, minor aggregation of the NPs in the colloid **QD1-1-3** occurs. Apparently, the molecules of main ligand **1** per se are long and flexible enough to be ordered by LC molecules (cf. Figure 5b and d). Furthermore, the distorted topology of the individual surfactant **1** within the shell leaves a space of low surfactant density around the equatorial region of the QD, which facilitates interactions between NPs and therefore ultimately leads to aggregate formation; a schematic representation of such an aggregate structure is shown in Figure 5c.

In further agreement with our model, a large degree of aggregation was observed in the dispersions of QDs decorated with individual dendritic surfactant **2**. The conic shape of the ligand leads to a dense packing of the surfactant molecules on the surface of the particle (Figure 5d), thereby preventing penetration of the constituent molecules of the LC host into

dx.doi.org/10.1021/la401475b | *Langmuir* 2013, 29, 9301–9309

the NP shell and limiting the flexibility of the dendritic surfactant. Similar limitation of the ligand flexibility was observed in dispersions of Au NPs covered with individual cyanobiphenyl surfactant in a nematic host.[61] Thus, in the case of **QD1-2**, the distortion of the local LC ordering is strong and aggregation of the particles is observed with a degree of aggregation similar to that of QDs grafted with native surfactant (**QD2**).

CONCLUSIONS

Our studies clearly show that the optimization of the interactions between a LC host and nanoparticles by minimization of the distortion of the local LC ordering is a practical method for the preparation of thermodynamically stable colloids of nanoparticles in nematic LC matrixes. Minimization of the LC distortion is achieved by preparation of the QDs shell structure that provides (i) effective penetration of the constituent molecules of the LC host into the surfactant layer and (ii) effective interaction between LC host and the surfactant molecules, which results in the adjustment of ligand ordering to match the ordering of the surrounding LC. The ratio of the concentrations of the main surfactant and the cosurfactant plays an important role in determining the strength of the LC−NP interactions, as is the relative lengths of the two employed surfactants. The optimization of these values is necessary in order to produce enough room for the penetration of the LC host molecules into the NP's shell and to provide an angular mobility of the main surfactant molecules. Certainly, the study of the full range of QDs concentration in LC is an important issue and this is planned for our further work.

The luminescence of QDs allowed us to monitor a degree of aggregation in the colloids of QDs covered with different surfactants and to demonstrate the validity of our approach. Specifically, we found that coating of QDs with the mixture of long-length dendrite promesogenic surfactant and the short-length aliphatic cosurfactant results in a "true" colloid of the QDs in a 5CB.

The suggested strategy can be further extended to the creation of thermodynamically stable colloidal dispersions of nanoparticles of different chemical constitutions/properties (e.g., metals, ferroelectrics, ferromagnetics, dielectrics, etc). This promises to solve the problem of the aggregation of nanoparticles in thermotropic LCs, and opens the way for the future application of LC colloids in a variety of advanced devices.

ASSOCIATED CONTENT

Supporting Information

Description of general methods, synthetic protocols for surfactant **2** syntheses, site-exchange procedure of QDs accompanied with corresponding FT-IR spectral evolutions, TEM images of QDs, statistical analysis of the distances between centers of NPs, estimation of the average distance between nanoparticles for their 0.25 wt % dispersions in 5CB, and description of the FCS procedure. This material is available free of charge via the Internet at http://pubs.acs.org.

AUTHOR INFORMATION

Corresponding Author

*Mailing address: Department of Technology of Organic Compounds, State Scientific Institution "Institute for Single Crystals", National Academy of Sciences of Ukraine, Lenin Ave, 60, Kharkov, 61001, Ukraine. Tel.: +38 044 3410128. E-mail: valeravv@isc.kharkov.com.

Author Contributions

The manuscript was written through contributions of all authors. All authors have given approval to the final version of the manuscript.

Notes

The authors declare no competing financial interest.

ACKNOWLEDGMENTS

Financial supports from the Royal Society (International Incoming Short Visits 2008/R1) and National Academy of Science of Ukraine (Projects #0110U003977, #0109U008051 and research fellowship #288-12.10.2011), STCU-NASU (Project #5205), and ARCUS program (collaboration of Ukraine, Russia and region Alsace) are gratefully acknowledged. We thank to Dr. Chernyshuk for the valued and fruitful discussions and to L. Richert for help with FCS analysis.

REFERENCES

(1) Hegmann, T.; Qi, H.; Marx, V. M. Nanoparticles in liquid crystals: synthesis, self-assembly, defect formation and potential applications. *J. Inorg. Organomet. Polym. Mater.* **2007**, *17*, 483−508.
(2) Bisoyi, H. K.; Kumar, K. Liquid-crystal nanoscience: an emerging avenue of soft self-assembly. *Chem. Soc. Rev.* **2011**, *40*, 306−319.
(3) Gardner, D. F.; Evans, J. S.; Smalyukh, I. I. Towards reconfigurable optical metamaterials: colloidal nanoparticle self-assembly and self-alignment in liquid crystals. *Mol. Cryst. Liq. Cryst.* **2011**, *545*, 1227−1245.
(4) Stamatoiu, O.; Mirzaei, J.; Feng, X.; Hegmann, T. Nanoparticles in Liquid Crystals and Liquid Crystalline Nanoparticles. *Top. Curr. Chem.* **2012**, *318*, 331−394.
(5) Mirzaei, J.; Reznikov, M.; Hegmann, T. Quantum dots as liquid crystal dopants. *J. Mater. Chem.* **2012**, *22*, 22350−22365.
(6) Brochard, F.; de Gennes, P. G. Theory of magnet suspension in liquid crystals. *J. Phys. (Paris)* **1970**, *31*, 691−708.
(7) Chen, S. H.; Amer, N. M. Operation of macroscopic collective behavior and new texture in magnetically dopped liquid crystals. *Phys. Rev. Lett.* **1983**, *51*, 2298−2301.
(8) Reznikov, Y.; Buchnev, O.; Tereshchenko, O.; Reshetnyak, V.; Glushchenko, A.; West, J. Ferroelectric nematic suspension. *Appl. Phys. Lett.* **2003**, *82*, 1917−1919.
(9) Čopič, M.; Mertelj, A.; Buchnev, O.; Reznikov, Yu. Coupled director and polarization fluctuations in suspensions of ferroelectric nanoparticles in nematic liquid crystals. *Phys. Rev. E* **2007**, *76*, 011702.
(10) Kopcansky, P.; Tomasovicova, N.; Timko, M.; Koneracka, M.; Zavisova, V.; Tomčo, L.; Jadzyn, J. The sensitivity of ferronematics to external magnetic fields. *J. Phys. (Paris)* **2010**, *200*, 72055.
(11) Hu, W.; Zhao, H.; Shan, L.; Song, L.; Cao, H.; Yang, Zh.; Cheng, Z.; Li, S.; Yang, H.; Guo, L. Magnetite nanoparticles/chiral nematic liquid crystal composites with magnetically addressable and magnetically erasable characteristics. *Liq. Cryst.* **2010**, *37*, 563−569.
(12) Buluy, O.; Burseva, D.; Hakobyan, M. R.; Goodby, J. W.; Kolosov, M. A.; Reznikov, Yu.; Hakobyan, R. S.; Slyusarenko, K.; Prodanov, M. F.; Vashchenko, V. V. Influence of Surface Treatment of Ferromagnetic Nanoparticles on Properties of Thermotropic Nematic Liquid Crystals. *Mol. Cryst. Liq. Cryst.* **2012**, *560*, 149−158.
(13) Kaczmarek, K.; Buchnev, O.; Nandhakumar, I. Ferroelectric nanoparticles in low refractive index liquid crystals for strong electro-optic response. *Appl. Phys. Lett.* **2008**, *92*, 103307.
(14) Liang, H.-H.; Xiao, Y.-Z.; Hsh, F.-J.; Wu, C.-C.; Lee, J.-Y. Enhancing the electro-optical properties of ferroelectric liquid crystals by doping ferroelectric nanoparticles. *Liq. Cryst.* **2010**, *37*, 255−261.
(15) Gupta, M.; Satpathy, I.; Roy, A.; Pratibha, R. Nanoparticle induced director distortion and disorder in liquid crystal-nanoparticle dispersions. *J. Colloid Interface Sci.* **2010**, *352*, 292−298.

(16) Marx, V. M.; Girgis, H.; Heiney, P. A.; Hegmann, T. Bent-core liquid crystal (LC) decorated gold nanoclusters: synthesis, self-assembly, and effects in mixtures with bent-core LC hosts. *J. Mater. Chem.* **2008**, *18*, 2983−2994.
(17) Urbanski, M.; Kinkead, B.; Hegmann, T.; Kitzerow, H.-S. Director field of birefringent stripes in liquid crystal/nanoparticle dispersions. *Liq. Cryst.* **2010**, *37*, 1151−1156.
(18) Khatua, S.; Manna, P.; Chang, W.-S.; Tcherniak, A.; Friedlander, E.; Zubarev, E. R.; Link, S. Plasmonic nanoparticles-liquid crystal composites. *J. Phys. Chem. C* **2010**, *114*, 7251−7257.
(19) Draper, M.; Saez, I. M.; Cowling, S. J.; Gai, P.; Heinrich, B.; Donnio, B.; Guillon, D.; Goodby, J. W. Self-Assembly and shape morphology of liquid crystalline gold metamaterials. *Adv. Funct. Mater.* **2011**, *21*, 1260−1278.
(20) Milette, J.; Cowling, S. J.; Toader, V.; Lavigne, C.; Saez, I. M.; Lennox, R. B.; Goodby, J. W.; Reven, L. Reversible long range network formation in gold nanoparticle-nematic liquid crystal composites. *Soft Matter* **2012**, *8*, 173−179.
(21) Soule, E. R.; Milette, J.; Reven, L.; Rey, A. D. Phase equilibrium and structure formation in gold nanoparticles-nematic liquid crystal composites: experiments and theory. *Soft Matter* **2012**, *8*, 2860−2866.
(22) Qi, H.; Kinkead, B.; Marx, V. M.; Zhang, H. R.; Hegmann, T. Miscibility and Alignment Effects of Mixed Monolayer Cyanobiphenyl Liquid-Crystal-Capped Gold Nanoparticles in Nematic Cyanobiphenyl Liquid Crystal Hosts. *Chem. Phys. Chem.* **2009**, *10*, 1211−1218.
(23) Williams, Y.; Chan, K.; Park, J. H.; Khoo, I. Ch.; Lewis, B.; Mallouk, T. E. Electro-optical and nonlinear optical properties of semiconductor nanorod doped liquid crystals. *Proc. SPIE* **2005**, 593−613.
(24) Wu, K.-J.; Chu, K.-C.; Chao, C.-Y.; Chen, Y.-F. CdS nanorods imbedded in liquid crystal cells for smart optoelectronic devices. *Nano Lett.* **2007**, *7*, 1908−1913.
(25) Williams, Y. Zh.; Lewis, B.; Mallouk, T. Photorefractive CdSe and gold nanowire-doped liquid crystals and polymer-dispersed-liquid-crystal photonic crystals. *Mol. Cryst. Liq. Cryst.* **2006**, *446*, 233−244.
(26) Shoute, L. C. T.; Kelley, D. F. Spatial organization of GaSe quantum dots: organic/semiconductor liquid crystals. *J. Phys. Chem. C* **2007**, *111*, 10233−10239.
(27) Tong, X.; Zhao, Y. Liquid-crystal gel-dispersed quantum dots: reversible modulation of photoluminescence intensity using an electric field. *J. Am. Chem. Soc.* **2007**, *129*, 6372−6373.
(28) Shandryuk, G. A.; Matukhina, E. V.; Vasil'ev, R. B.; Rebrov, A.; Bondarenko, G. N.; Merekalov, A. S.; Gas'kov, A. M.; Talroze, R. V. Effect of H-bonded liquid crystal polymers on CdSe quantum dot alignment within nanocomposite macromolecules. *Macromolecules* **2008**, *41*, 2178−2185.
(29) Danilov, V. V.; Artem'ev, M. V.; Baranov, A. V.; Yermolayeva, G. M.; Utkina, N. A.; Khrebtov, A. I. Fluorescence of semiconductor nanorods in liquid-crystal composites. *Opt. Spectrosc.* **2008**, *105*, 306−309.
(30) Basu, R.; Iannacchione, G. S. Evidence for directed self-assembly of quantum dots in a nematic liquid crystal. *Phys. Rev. E* **2009**, *80*, 10701.
(31) Hirst, L. S.; Kirchhoff, J. H.; Inman, R. H.; Ghosh, S. Quantum dot self-assembly in liquid crystal media. *Proc. SPIE* **2010**, *7618*, 76180f.
(32) Kinkead, B.; Hegmann, T. Effects of size, capping agent, and concentration of CdSe and CdTe quantum dots doped into a nematic liquid crystal on the optical and electro-optic properties of the final colloidal liquid crystal mixture. *J. Mater. Chem.* **2010**, *20*, 448−458.
(33) Surpo, N. A.; Vakshtein, M. S.; Kamanina, N. V. Effect of CdSe/ZnS semiconductor quantum dots on the dynamic properties of nematic liquid-crystalline medium. *Tech. Phys. Lett.* **2010**, *36*, 319−321.
(34) Chen, H.-S.; Chen, Ch.-W.; Wang, C.-H.; Chu, F.-Ch.; Chao, C.-Y.; Kang, Ch.-Ch; Chou, P.-T.; Chen, Y.-F. Color-tunable light-emitting device based on the mixture of CdSe nanorods and dots embedded in liquid-crystal cells. *J. Phys. Chem. C* **2010**, *114*, 7995−7998.
(35) Verma, Y. K.; Inman, R. H.; Ferri, C. G.; Mirafzal, H.; Ghosh, S. N.; Kelley, D. F.; Hirst, L. S.; Ghosh, S. Electrical modulation of static and dynamic spectroscopic properties of coupled nanoscale GaSe quantum dot assemblies. *Phys. Rev. B* **2010**, *82*, 165428.
(36) Vasilets, V. N.; Savenkov, G. N.; Merekalov, A. S.; Shandryuk, G. A.; Shatalova, A. M.; Tal'roze, R. V. Immobilization of quantum dots of cadmium selenide on the matrix of a graft liquid-crystalline polymer. *Polym. Sci., Ser. A* **2011**, *52*, 521−526.
(37) Chen, Ch.-T.; Liu, Ch.-Ch.; Wang, Ch.-H.; Chen, Ch.-W.; Chen, Y.-F. Tunable coupling between exciton and surface plasmon in liquid crystal devices consisting of Au nanoparticles and CdSe quantum dots. *Appl. Phys. Lett.* **2011**, *98*, 261918.
(38) Mirzaei, J.; Urbanski, M.; Yu, K.; Kitzerow, H.-S.; Hegmann, T. Nanocomposites of a nematic liquid crystal doped with magic-sized CdSe quantum dots. *J. Mater. Chem.* **2011**, *21*, 12710−12716.
(39) Kumar, A.; Biradar, A. M. Effect of cadmium telluride quantum dots on the dielectric and electro-optical properties of ferroelectric liquid crystals. *Phys. Rev. E* **2011**, *83*, 41708.
(40) Lapanik, A.; Rudzki, A.; Kinkead, B.; Qi, H.; Hegmann, T.; Haase, W. Electrooptical and dielectric properties of alkylthiol-capped gold nanoparticle−ferroelectric liquid crystal nanocomposites: influence of chain length and tethered liquid crystal functional groups. *Soft Matter* **2012**, *8*, 8722−8728.
(41) Szilágyi, A.; Fetter, G.; Zrínyi, M. Thermotropic behaviour of the complex liquid crystal system containing 8CB [4-cyano-4′-(n-octylbiphenyl)] and organic ferrofluid. *J. Therm. Anal. Calorim.* **2005**, *82*, 525−530.
(42) Da Cruz, C.; Sandre, O.; Cabuil, V. Phase behavior of nanoparticles in a thermotropic liquid crystal. *J. Phys. Chem. B* **2005**, *109*, 14292−14299.
(43) Prodanov, M. F.; Kolosov, M. A.; Krivoshey, A. I.; Fedoryako, A. P.; Yarmolenko, S. N.; Semynozhenko, V. P.; Goodby, J. W.; Vashchenko, V. V. Dispersion of magnetic nanoparticles in polymorphic liquid crystal. *Liq. Cryst.* **2012**, *39*, 1512−1526.
(44) Chernyshuk, S.; Lev, B.; Yokoyama, H. Paranematic interaction between nanoparticles of ordinary shape. *Phys. Rev. E* **2005**, *71*, 062701.
(45) Bae, W. K.; Char, K.; Hur, H.; Lee, S. Single-step synthesis of quantum dots with chemical composition gradients. *Chem. Mater.* **2008**, *20*, 531−539.
(46) Kopping, J. T.; Patten, T. E. Identification of acidic phosphorus-containing ligands involved in the surface chemistry of CdSe nanoparticles prepared in tri-N-octylphosphine oxide solvents. *J. Am. Chem. Soc.* **2008**, *130*, 5689−5698.
(47) Goodby, J. W.; Saez, I. M.; Cowling, S. J.; Gasowska, Ju. S.; MacDonald, R. A.; Sia, S.; Watson, P.; Toyne, K. J.; Hird, M.; Lewis, R.; Lee, S.-E.; Vaschenko, V. Molecular complexity and the control of self-organising processes. *Liq. Cryst.* **2009**, *36*, 567−605.
(48) Talapin, D. V.; Lee, J.-S.; Kovalenko, M. V.; Shevchenko, E. V. Prospects of colloidal nanocrystals for electronic and optoelectronic applications. *Chem. Rev.* **2010**, *110*, 389−458.
(49) Green, M. The nature of quantum dot capping ligands. *J. Mater. Chem.* **2010**, *20*, 5797−5809.
(50) Munro, A. M.; Plante, I. J.-L.; Ng, M. S.; Ginger, D. S. Quantitative study of the effects of surface ligand concentration on CdSe nanocrystal photoluminescence. *J. Phys. Chem. C* **2007**, *111*, 6220−6227.
(51) Zhao, Y.; Li, Y.; Song, Y.; Jiang, W.; Wu, Zh.; Wang, A.; Sun, J.; Wanga, J. Architecture of stable and water-soluble CdSe/ZnS core-shell dendron nanocrystals via ligand exchange. *J. Colloid Interface Sci.* **2009**, *339*, 336−343.
(52) Morris-Cohen, A. J.; Donakowski, M. D.; Knowles, K. E.; Weiss, E. A. The Effect of a Common Purification Procedure on the Chemical Composition of the Surfaces of CdSe Quantum Dots Synthesized with Trioctylphosphine Oxide. *J. Phys. Chem. C* **2010**, *114*, 897−906.
(53) Dertinger, T.; Pacheco, V.; Hocht, I.; Hartmann, R.; Gregor, I.; Enderlein, J. Two-Focus Fluorescence Correlation Spectroscopy: A New Tool for Accurate and Absolute Diffusion Measurements. *Chem. Phys. Chem.* **2007**, *8*, 433−443.

(54) Jadzyn, J.; Dambrowski, R.; Lech, T.; Czechowski, G. Viscosity of the Homologous Series of n-Alkylcyanobiphenyls. *J. Chem. Eng. Data* **2001**, *46*, 110−112.
(55) Sabet, R. A.; Khoshsima, H. Real-time holographic investigation of azo dye diffusion in a nematic liquid crystal host. *Dyes Pigm.* **2010**, *87*, 95−99.
(56) Heuff, R. F.; Swift, J. L.; Cramb, D. T. Fluorescence correlation spectroscopy using quantum dots: Advances, challenges and opportunities. *Phys. Chem. Chem. Phys.* **2007**, *9*, 1870−1880.
(57) Clamme, J. P.; Azoulay, J.; Mely, Y. Monitoring of the formation and dissociation of polyethylenimine/DNA complexes by two photon fluorescence correlation spectroscopy. *Biophys. J.* **2003**, *84*, 1960−1968.
(58) Cseh, L.; Mehl, G. H. The Design and Investigation of Room Temperature Thermotropic Nematic Gold Nanoparticles. *J. Am. Chem. Soc.* **2006**, *128*, 13376−13377.
(59) Wojcik, M.; Lewandowski, W.; Matraszek, J.; Mieczkowski, J.; Borysiuk, J.; Pociecha, D. Liquid-Crystalline Phases Made of Gold Nanoparticles. *Angew. Chem., Int. Ed.* **2009**, *48*, 5167−5169.
(60) Qi, H.; Hegmann, T. Formation of periodic stripe patterns in nematic liquid crystals doped with functionalized gold nanoparticles. *J. Mater. Chem.* **2006**, *16*, 4197−4205.
(61) Milette, J.; Toader, V.; Soulé, E. R.; Lennox, R. B.; Rey, A. D.; Reven, L. A Molecular and Thermodynamic View of the Assembly of Gold Nanoparticles in Nematic Liquid Crystal. *Langmuir* **2013**, *29*, 1258−1263.